AIAA JOURNAL
Vol. 32, No. 10, October 1994

Experimental Investigation of Fringe Divergence Errors in Laser Velocimetry Measurements

Gary A. Fleming*
ViGYAN, Inc., Hampton, Virginia 23666
and
John M. Kuhlman†
West Virginia University, Morgantown, West Virginia 26506

The effects of fringe divergence on the accuracy of laser velocimetry measurements have been investigated experimentally to obtain data that is supportive of a previously published theory by Hanson. The theory has been generalized to show that a similarity solution in terms of the laser beam confocal parameter may be derived. Experimental results are in good agreement with the similarity profile, proving the validity of both the similarity parameter and the published theory. The theory is used to develop alignment criteria to avoid residual turbulence resulting from fringe divergence.

Nomenclature

b	= confocal parameter, confocal distance
C_1	= defined constant
C_η	= defined constant
F	= lens focal length
f	= signal burst frequency
I_R	= residual turbulence intensity
l_{pv}	= probe volume length (dimensional)
$R(z_b)$	= radius of curvature of light wave fronts constituting Gaussian laser beam
$w(z_b)$	= radius of Gaussian laser beam
w_0	= radius of beam waist
z	= distance along optical axis
z_b	= distance along laser beam propagation axis
z_0	= location of beam waist along optical axis
α	= cross beam half-angle
ζ	= defined parameter
η	= similarity parameter (defined)
η_{pv}	= nondimensional probe volume length
λ	= wavelength of laser light
ξ	= defined parameter
σ	= standard deviation

Introduction

FRINGE divergence and its effect on laser velocimetry (LV) measurements have been under theoretical consideration since the early 1970s. However, to date, only limited experimental data has been presented to validate these theories. The pioneering work concerning fringe divergence was performed by Hanson,[1] who derived an equation which predicted the magnitude of the interference plane gradients inside the LV measurement volume. Hanson also described an experimental method to measure these gradients, but did not provide enough experimental data to conclusively verify his theoretical results. Durst and Stevenson[2] also treated the problem of fringe divergence theoretically, performing manipulations of Hanson's original calculations. Additionally, Durst and Stevenson provided theoretical calculations intended to model a frequency "chirp," which occurs because of divergent fringe patterns. However, no experimental data was provided to demonstrate that these calculations quantitatively predicted the magnitude of errors caused by fringe divergence.

In an effort to acquire data that would verify the theory derived by Hanson and quantitatively assess the effects of fringe divergence, a preliminary experimental investigation was undertaken at NASA Langley Research Center, Hampton, Virginia. This experiment, performed by Langley personnel, led to results that were inconclusive as to whether or not the phenomenon of fringe divergence exists and if the theories describing fringe divergence are accurate. A second experimental effort that would (hopefully) lead to more conclusive results than those obtained at Langley has been undertaken at West Virginia University and will be discussed in this paper.

Causes and Concerns of Fringe Divergence

The premise behind fringe divergence in laser velocimetry is that, in general, the laser beams forming the LV probe volume do not intersect precisely at their beam waists (where the diameters of the beams are smallest). In most single component LV systems, the output beams that intersect to form the measurement volume are derived from a single input laser beam which is passed through a beamsplitter. The two resulting beams are then passed through a single lens that causes the beams to intersect at the lens focal point. The beam exiting the laser is divergent, and focusing the divergent beam results in light wave front distortion and a shift in the location of the focused beam's waist. For the focused beam, the light wave fronts are planar in an area surrounding the beam waist. Away from this region, the wave fronts become more spherical, with a radius of curvature that is dependent on the distance from the waist. If the beams intersect at their waists as shown schematically in Fig. 1a, the light wave fronts are planar, and optical interference planes are created which are evenly spaced and parallel. This is the "ideal" LV probe volume, since any seed particle passing through the probe volume at any position will be subject to the same fringe spacing. If the beams intersect at some distance away from the beam waists, the light wave fronts are spherical, and the optical interference planes that result are no longer evenly spaced and parallel. This is shown in Fig. 1b, which represents (in exaggerated fashion) two laser beams intersecting prior to the location of the waists. As a result of the nonuniform fringe spacing, measurement errors would be introduced since uniform fringe spacing is assumed for the conversion of frequency to velocity. The variation in velocity resulting from divergent fringes will add a residual turbulence (an artificial increase in the measured velocity standard

Received Nov. 1, 1993; presented as Paper 94-0043 at the AIAA 32nd Aerospace Sciences Meeting, Reno, NV, Jan. 10–13, 1994; revision received April 15, 1994; accepted for publication April 25, 1994.

*Research Engineer, 30 Research Drive.
†Professor, Department of Mechanical and Aerospace Engineering. Associate Fellow AIAA.

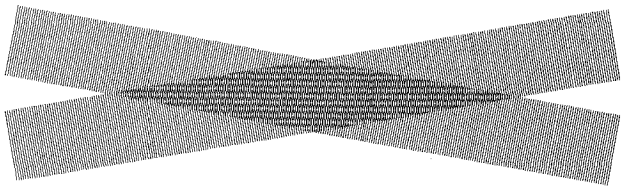

Fig. 1a Schematic of laser beams intersecting at waists.

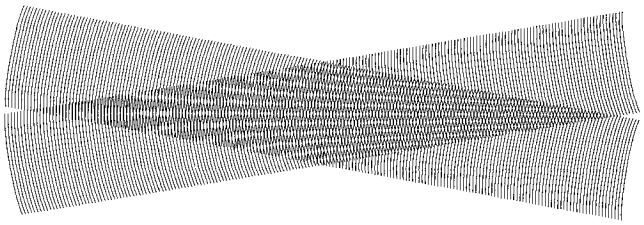

Fig. 1b Schematic of laser beams intersecting prior to waists.

deviation) to the measured ensemble statistics. For an impinging particle, the path followed by the particle as it passes through the probe volume cannot be determined. Therefore, it would be impossible to compensate for fringe divergence by applying other nonuniform fringe spacing schemes. Thus, the residual turbulence cannot be distinguished from the true flow turbulence. Because of this reason, it would be essential to minimize fringe divergence when accurate measurement of the flow turbulence quantities is desired.

The underlying assumption of the fringe divergence premise is that the probe volume length is shorter than the confocal distance b, defined as the distance over which the wave fronts may be considered planar. If this assumption was invalid, divergent fringes could occur on both sides of the probe volume simultaneously, and residual turbulence would be present even when the beams were crossed at their waists. Through a simple order of magnitude analysis of the quantity l_{pv}/b, it may be seen that this assumption will always be valid for all practical optical configurations.

If fringe divergence were to be present within a system, it would generally result from intersecting both beams either prior to or after the location of the beam waists. Durst and Stevenson[2] also treat the case where the beams intersect on opposing sides of the waists. This could only occur in nonoptically compensated systems, or systems using inexpensive optics and high powered lasers where thermal blooming of the optical components might occur. This would present a different phenomenon than that represented in Fig. 1b. However, it is extremely rare that this would occur since optical compensation has been incorporated into LV optical components since the measurement technique was invented. Additionally, all commercial LV optics are constructed of high quality components, preventing thermal blooming. For all practical purposes, beam intersections will always occur with both beams intersecting on the same side of their waists. Therefore, the present discussion will be limited to the case shown in Fig. 1b (and its mirror image), since the theory that is to be experimentally validated[1] is based on this configuration.

According to the theoretical predictions of Hanson, errors induced by divergent fringes are most likely negligible for typical LV measurement applications. However, this error source may become significant for some optical configurations, particularly those using beam expansion. If the theory is accurate, attention must be paid to minimize fringe divergence since residual turbulence caused by divergent fringes is not distinguishable from the true flow turbulence. Hanson's theoretical predictions[1] show that errors caused by fringe divergence reach a maximum when the laser beams are intersected at distances that are relatively close to the beam waist. If this is the case, a small error in optical alignment could lead to larger errors resulting from fringe divergence. The theory also shows that if the beams are intersected far away from the waists, errors resulting from divergent fringes are reduced. However, probe volume diameter is increased, causing a variety of other problems such as decreased signal-to-noise ratio and spatial resolution.

Prior to the present study, experiments to determine if the theoretical predictions of Hanson were correct had not been undertaken, and the accuracy of the theory had been unknown. Therefore, it was important to conduct experimental investigations to determine the validity of the theory, or if errors induced by fringe divergence could potentially be much more significant than what theory would predict. Experimental validation of Hanson's theory could also lead to a reliable guideline concerning the margin of error that researchers should follow in system alignment to ensure that errors caused by fringe divergence are minimized.

Theory

The first theoretical analysis concerning fringe divergence was performed by Hanson.[1] This derivation was based on two fundamental parameters, which are the radius of the laser beam $w(z_b)$ and the radius of curvature of the light wave fronts that constitute the beam $R(z_b)$, where z_b represents the distance (along the beam) from the beam waist. If the beam waist is assumed to be at $z_b = 0$, then the equations for the given parameters are[2]

$$w^2(z_b) = w_0^2\left[1+\left(\frac{\lambda z_b}{\pi w_0^2}\right)^2\right] \tag{1}$$

$$R(z_b) = z_b\left[1+\left(\frac{\pi w_0^2}{\lambda z_b}\right)^2\right] \tag{2}$$

Hanson showed that it was possible to derive an expression for the shift in signal burst frequency df as a function of the displacement of the scattering surface within the probe volume. Hanson found this expression to be

$$\frac{1}{f}\frac{df}{dz} = \frac{-1}{R(z)} \tag{3}$$

Note that in the derivation of Eq. (3) the cross beam half-angle is assumed small, and the small angle approximation is applied. Using further manipulations, Durst and Stevenson derived the expression

$$\frac{F}{f}\frac{df}{dz} = \frac{z_0 - F}{F} \tag{4}$$

which expresses the gradient of the interference planes as a function only of the lens focal length F and the crossing distance away from the beam waist $(z_0 - F)$.

Further manipulations may be performed to derive a similarity solution for the interference plane gradients. Using Eq. (2) in Eq. (3) yields

$$\frac{1}{f}\frac{df}{dz} = \frac{-[(z-z_0)]}{(z-z_0)^2 + C_1^2}, \qquad C_1 = \frac{\pi w_0^2}{\lambda} \tag{5}$$

To nondimensionalize this equation, a similarity parameter η has been defined as

$$\eta = (z - z_0)/b \tag{6}$$

where b is the beam confocal parameter. Physically, the confocal parameter is the distance along the beam, symmetric about the beam waist, over which the beam may be considered almost perfectly collimated. In this region, the light wave fronts within the beam are almost perfectly planar. An expression for the confocal parameter is[3]

$$b = \frac{8\pi w_0^2}{\lambda} = 8C_1 \tag{7}$$

where C_1 has been defined in Eq. (5). The similarity parameter η physically represents the percentage of the confocal distance at which the beam intersection $(z - z_0)$ is occurring. If the expressions for η and b are used in Eq. (5), the equation for the interference plane gradients may be expressed as

$$\frac{1}{f}\frac{df}{d\eta} = \frac{-\eta}{\eta^2 + 1/64} \tag{8}$$

Note that Eq. (8) is now in nondimensional form. Recall that the small angle approximation has been applied to the cross beam half-angle in the derivation of Eq. (3). If the cross beam half-angles are small enough so that the small angle approximation can be made, this nondimensionalization leads to a similarity solution describing the interference plane gradients. Approximate similarity is maintained for optical systems with moderate cross beam angles. Equation (8) has been graphed in Fig. 2. To demonstrate that Eq. (8) does lead to a similarity profile for all optical configurations, the equation has been plotted using three different sets of optical parameters. These sets of parameters are listed in Table 1, and the resulting plot is shown in Fig. 3. Despite differences in optical configurations, Fig. 3 shows that all of the profiles describe the same, single curve, indicating similarity and, thus, the validity of the similarity parameter η.

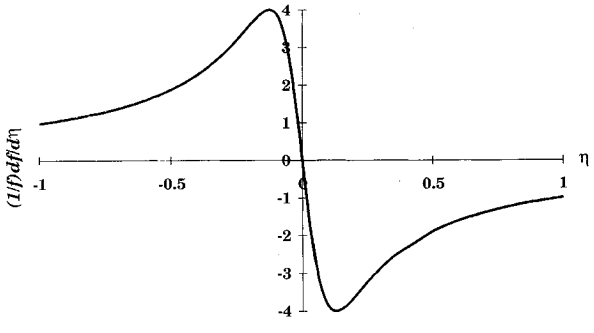

Fig. 2 Theoretical similarity profile.

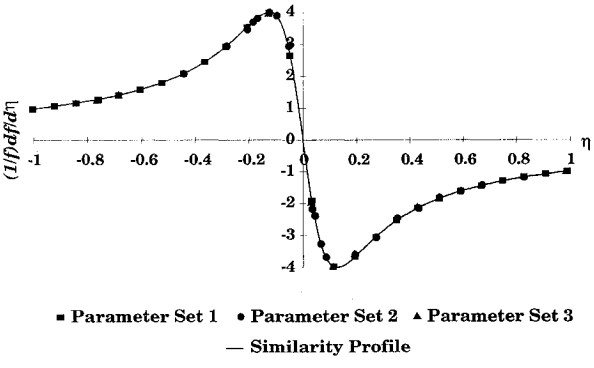

▪ Parameter Set 1 • Parameter Set 2 ▲ Parameter Set 3

— Similarity Profile

Fig. 3 Nondimensionalization of the interference plane gradients for three different sets of optical parameters; see Table 1 for parameter values.

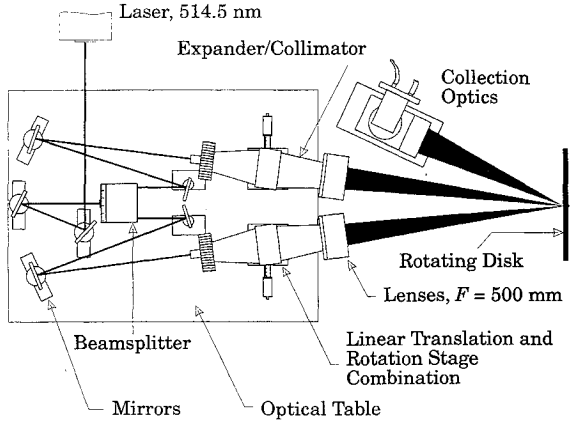

Fig. 4 Experimental setup.

The maximum magnitude of the similarity profile occurs at $|\eta| = 0.125$, where $|(1/f)(df/d\eta)| = 4$. This indicates to minimize the effects of fringe divergence, alignment should be performed to ensure that the beams intersect at locations that lie well within ±12.5% of the confocal distance away from the beam waist. For most LV systems, alignment to this degree of accuracy is easily accomplished. However, alignment to this degree of accuracy in systems with short confocal parameters may be difficult to achieve. Alignment could also be performed so that the beams intersect at distances greater than the confocal distance away from the beam waist ($|\eta| \geq 1$). As discussed previously, although fringe divergence is reduced, errors induced by increased probe volume diameter become prevalent at these positions. For systems using high power lasers, the signal-to-noise ratio can be increased by increasing laser power. For low power systems, however, it is not recommended that the beams be intersected at these positions in order to reduce the amount of fringe divergence. In either case, the loss of spatial resolution cannot be recovered.

For LV systems using zoom lenses, it may actually be beneficial to intersect the laser beams at a location far away from the beam waists. Because the zoom lens focuses the beams at a variety of crossing locations, the distance between the lens focal point and the focused beam waist location will not remain constant at each position of the zoom lens. Aligning the system so that the beams initially intersect at some location far away from the beam waist allows for a greater variation in the allowable distance between the lens focal point and the beam waists. This reduces the probability that the intersection will occur at a location where fringe divergence is maximized.

Experimental Verification

The purpose of the experiments was to acquire data indicating the validity of the fringe divergence premise and nondimensionalization expressed by Eq. (8). An LV system was configured so that any error sources resulting from fringe divergence would be relatively easy to discern. The amount of adjustability that was desired from the optics precluded the use of conventional configurations such as a dual beam, single lens system. A system was constructed that made it possible to vary the beam confocal distance and crossing location, which were the primary parameters of interest. To maintain a constant cross beam angle, beam spacing was changed to translate the beam crossing location along the optical axis. The system used is shown schematically in Fig. 4. Table 1, set 3 lists the optical parameters for the experimental setup. The entire optical configuration (not including collection optics) fit on a 46 × 61 cm aluminum plate which served as an optical mounting table. The expander/collimators provide two expansion settings, the largest of which (approximately 19.2) was chosen. The large expansion ratio was chosen to accentuate the potential error source and to determine if the fringe divergence results obtained for such a system would collapse to the similarity profile given by Eq. (8).

Table 1 Optical parameters used to show similarity for Eq. (8)

Parameter	Set 1	Set 2	Set 3
Wavelength, nm	476.5	488.0	514.5
Cross beam angle, deg	1.2	2.5	6.5
Beam expansion	11.0	1.0	19.2
Beam diameter at laser aperture, mm	1.3	1.3	1.3
Beam divergence exiting aperture, mrad	0.6	0.6	0.6
Distance from laser aperture to lens, m	3.00	1.00	1.91
Lens focal length, m	4.00	1.00	0.50
Calculated confocal distance, m	0.63	4.35	0.003
Calculated probe volume length (at waists), mm	8.1	10.8	0.1

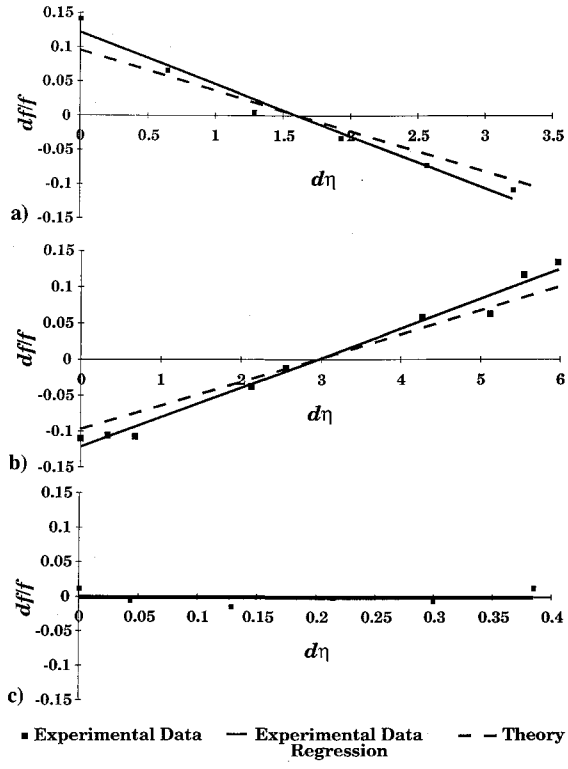

Fig. 5 Measurement of the interference plane gradients when beams were intersected at a) $\eta = +16.8$, b) $\eta = -30.3$, and c) $\eta = 0$.

Procedure

To acquire pertinent data, it was desired to intersect the two incident laser beams that form the probe volume symmetrically at different distances along the optical axis. In this manner, the nondimensional parameter η could be varied. At each intersection location, a black anodized aluminum disk rotating at a constant angular frequency was placed perpendicular to the interference planes. Having effectively zero thickness, a solid disk (rather than translucent) was used because it provided a flat, definitive scattering surface. The disk angular velocity was set moderately low to minimize any vibrations that may have been present from imbalances of the disk. The probe volume was situated on the disk approximately 4 cm (30% total radius) vertically above the motor hub to minimize effects of wheel fluctuations occurring along the length of the probe volume. The disk was mounted to a linear translation stage equipped with a micrometer barrel, so that the disk could be incrementally traversed along the optical axis through the probe volume. The incremental distances over which the disk was moved varied depending on the length of the probe volume, but the disk was typically located at 6–8 different positions spanning the probe volume length. At each position of the disk within the probe volume, four ensemble frequency measurements, each consisting of 4096 samples, were taken and averaged to determine the average frequency at that disk location. The large amount of data was taken to minimize measurement statistical uncertainty. Each measurement was taken over approximately the same time record, and aperture times were used to reduce the data rate to approximately 400 samples/s. This slower data rate ensured that the ensemble measurements were acquired over a large number of disk rotations.

Following final adjustments, data was taken at beam crossing locations within −10 cm prior to the occurrence of the beam waists to +10 cm after the occurrence of the beam waists in 1-cm increments. This corresponded to η values ranging from ±33, so that the full nondimensional profile was included. Additional data points were taken at locations close to the beam waists to explore the shape of the peaks in the nondimensional profile of $(1/f)df/d\eta$ for ranges of $|\eta| \leq 1$. These additional data points were taken in 1-mm increments from −5 mm from the beam waists to +5 mm from the beam waists. Reference 4 includes further details of the experimental apparatus and procedure.

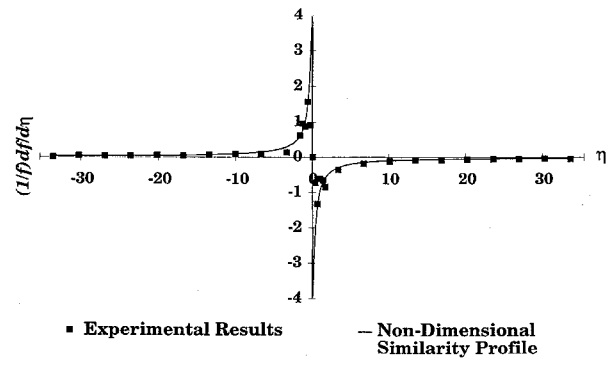

Fig. 6 Comparison between present experimental results and present similarity form of Hanson's theory, Eq. (8).

Results

Hanson[1] published results that showed the interference plane gradients within the probe volume were linear for the two measurement locations analyzed. This result has been found to be true for the present experiment. At every measurement location along the optical axis, the interference plane gradients were found to be very nearly linear. Figures 5a–5c show typical plots of the normalized measured mean frequency vs the nondimensional position of the disk within the probe volume for three separate positions along the optical axis. Theoretical predictions are also provided for comparative purposes. The data presented in Figs. 5a–5c was taken at crossing locations of $\eta = +16.8, -30.3$, and 0, respectively, and is representative of the data taken at other crossing locations along the optical axis. In Figs. 5a and 5b, there is a noticeable difference between the data slope magnitude and sign, resulting from the difference in crossing distance at which the data was acquired. Figure 5c shows the mean frequency data acquired by traversing the disk through the probe volume when the beams were intersected at the waists. Again, the data is approximately linear, with virtually zero slope, affirming that at this location the interference planes in the probe volume are parallel. The standard deviation magnitude was approximately 1.3% of the mean for all measurements, which is much smaller than the observed change in frequency as a function of disk position within the probe volume (except for the case presented in Fig. 5c, where the slope is approximately zero). Therefore, changes in the measured frequencies are much greater than the measurement statistical uncertainty, and must be the result of a physical phenomenon. As is evident from the data presented in Figs. 5a–5c, the experimental data and theoretical predictions match well.

To further assess the validity of the theory, normalization of the data in terms of the similarity parameter η was undertaken. First, the crossing distances from the beam waist were normalized by the confocal distance to obtain values of η. The quantities dz which represented the position of the disk inside the probe volume were also normalized by the confocal parameter to express these distances in terms of $d\eta$. To calculate the quantity $df/d\eta$, which is representative of the interference plane gradients, a linear regression was applied to each normalized data set taken at different intersection positions along the optical axis. The slopes resulting from the regressions yielded the quantity $df/d\eta$. The quantity $df/d\eta$ was normalized by the average frequency measured when the probe volume was formed at the beam waist to obtain the quantity $(1/f)(df/d\eta)$.

Figure 6 shows a plot of the nondimensionalized experimental data and the theoretical nondimensional similarity profile expressed by Eq. (8). As is evident from Fig. 6, the experimental data is very supportive of the theory. The actual maximum magnitude of the quantity $|(1/f)(df/d\eta)|$ measured was nominally 1.5, observed at crossing distances of ±2 mm from the beam waists. Although theoretical predictions show that the peak values of $|(1/f)(df/d\eta)|$ could reach as high as 4, alignment to cross the

beams at the exact locations where these peaks occur would have been extremely difficult. However, since the experimental data follows the theoretical profile so well in all other areas of the data, it is felt that it is very likely that values of $|(1/f)(df/d\eta)|$ do reach magnitudes up to 4 when the beams are intersected precisely at $\eta = \pm 0.125$.

During the course of performing the experiment and analysis of the data it became quite apparent that fringe divergence does exist. During the experiment, at some measurement locations along the optical axis, changes in frequency as a function of disk position within the probe volume could be visually observed on an oscilloscope. The data resulting from the experiments, when nondimensionalized, matches theoretical predictions well and confirms the validity of the similarity profile and Hanson's theoretical equation. Therefore, for any conventional optical configuration, the magnitude of fringe divergence as a function of beam crossing location may be expressed nondimensionally using Eq. (8).

Alignment Criteria

As discussed previously, one of the primary effects of fringe divergence is the superposition of a residual turbulence in the data. Although the alignment criteria of intersecting the beams well within 12.5% of the confocal distance from the beam waist serves well as a general guideline to minimize fringe divergence, it was desired to derive an expression that yielded definitive permissible margins of error for alignment. The following derivation, based on Eq. (8), leads to a relatively simple equation that allows the user to calculate these permissible margins of error.

It is first assumed that the beams are crossed at some location η and that the value of $(1/f)df/d\eta$ for that crossing location is known. Since $(1/f)df/d\eta$ is constant at crossing location η, this constant may be denoted by C_η and Eq. (8) may be written as

$$\frac{1}{f}\frac{df}{d\eta} = C_\eta \tag{9}$$

Assuming a uniform flow with constant velocity, the frequency f is the mean frequency that would be generated by multiple particles passing through the probe volume at random locations. At any particular crossing location, this mean frequency is constant. Therefore, Eq. (9) may be integrated over the length of the probe volume

$$\frac{1}{f}\int_{-\eta_{pv}}^{\eta_{pv}} df(\eta) = C_\eta \int_{-\eta_{pv}}^{\eta_{pv}} d\eta \tag{10}$$

where $\eta_{pv} = (l_{pv}/2)/b$. Performing the integration, it follows that

$$\frac{f(\eta_{pv}) - f(-\eta_{pv})}{f} = C_\eta(2\eta_{pv}) = C_\eta\left(\frac{l_{pv}}{b}\right) \tag{11}$$

Now, a constant velocity flow with uniform seed particle density is assumed. If it is assumed (temporarily) that the probability of particle measurement along the length of the probe volume is constant, a uniform frequency/occurrence distribution (histogram) will result from the passage of an ensemble of seed particles through the probe volume because of the linear growth in fringe spacing. Superimposed on this uniform distribution is a distribution governing the probability of particle measurement along the length of the probe volume, which is assumed to be Gaussian and equal to the light intensity profile along the probe volume length. The probe volume length is defined by the $1/e^2$ intensity points, corresponding to $\pm 2\sigma$ of the full intensity profile. Therefore, the frequencies that would be generated by particles passing through the $1/e^2$ intensity points [i.e., $f(\eta_{pv})$ and $f(-\eta_{pv})$] must also correspond to $\pm 2\sigma$ of the potential measured frequency range. From this, it may be seen that the left-hand side of Eq. (11) is equal to $4\sigma/f$, or four times the residual turbulence intensity resulting from divergent fringes.

Table 2 Alignment criteria calculated from Eqs. (13–15) for an allowable 1% residual turbulence intensity

Alignment value	Set 1	Set 2	Set 3
$\lvert\eta\rvert_{min}$	0.059	NA	0.019
$\lvert\eta\rvert_{max}$	0.263	NA	0.811
$\lvert(z-z_0)\rvert_{min,\,mm}$	37.3	NA	0.06
$\lvert(z-z_0)\rvert_{max,\,mm}$	165.2	NA	2.41
Maximum I_R, %	1.29	0.25	3.32

If a maximum permissible value of the residual turbulence intensity is assumed, the quantity C_η may be solved for. This subsequently leads to a determination of the crossing distances η which must be adhered to in order to maintain residual turbulence intensity levels lower than the maximum permissible value. Denoting the residual turbulence intensity as I_R, it follows that

$$C_\eta = \frac{4I_R b}{l_{pv}} = \frac{1}{f}\frac{df}{d\eta} = \frac{-\eta}{\eta^2 + 1/64} \tag{12}$$

Solving for η, Eq. (12) may be written as

$$\eta = \frac{-\xi \pm \sqrt{\xi^2 - 1/16}}{2}, \qquad \xi = \frac{l_{pv}}{4I_R b} \tag{13}$$

In its dimensional form, Eq. (13) becomes

$$z - z_0 = \frac{-\zeta \pm \sqrt{\zeta^2 - (b/4)^2}}{2}, \qquad \zeta = \frac{l_{pv}}{4I_R} \tag{14}$$

Equations (13) and (14) yield the margins of alignment error $|\eta|$ and $|(z-z_0)|$ that must be achieved to ensure residual turbulence intensities caused by fringe divergence are less than I_R.

Equations (13) and (14) have been applied using each of the parameter sets shown in Table 1 for a permissible residual turbulence intensity of 1%. The maximum alignment error values produced from these equations are listed in Table 2. No values are presented for set 2 (typical of smaller commercial LV systems), since the maximum residual turbulence intensity is less than 1%. For these calculations, the probe volume length was calculated as if the beams were intersected at their waists and assumed constant. As the beam intersection location moves along the optical axis, the effective probe volume size will change. However, changes of the intersection location within 12.5% of the confocal parameter should not produce significant changes in the effective probe volume length. This assumption also leads to a more stringent alignment region to achieve the same permissible residual turbulence intensity, so that the equations produce conservative alignment values. Perhaps more important than the calculation of the permissible margins of alignment error is the calculation of the maximum residual turbulence intensity that can occur for a system. The maximum values of the residual turbulence intensity occur at $\eta = \pm 0.125$. Inserting $\eta = \pm 0.125$ into Eq. (12) and manipulating, Eq. (15) results

$$I_{R,max} = l_{pv}/b \tag{15}$$

Equation (15) shows that for systems having relatively small cross beam angles, the maximum residual turbulence intensity (associated with divergent fringes) that could occur within the system is well approximated by the probe volume length divided by the beam confocal distance. The maximum residual turbulence intensities for the optical configurations shown in Table 1 have been calculated and included in Table 2.

Conclusions

The experimental data that has been acquired is conclusive in showing that fringe divergence does exist and that the theoretical

predictions of Hanson are a quantitative predictor of the magnitude of divergence. Also, the theory has been generalized to show that a similarity solution may be achieved in terms of the similarity parameter η defined previously.

For most LV systems and applications, fringe divergence does not represent a significant error source since typical LV systems have large confocal distances. However, for low turbulence applications or for some optical configurations, errors from fringe divergence may become significant. To aid in minimizing these errors, equations have been derived which enable LV users to calculate the maximum permissible margins of alignment error that must be adhered to in order to obtain residual turbulence intensities that are less than a desired percentage. Additionally, an equation predicting the maximum residual turbulence intensity caused by divergent fringes for any particular optical configuration has been derived. Although there is no experimental data to directly confirm these equations at this time, it is felt that the equations are accurate since they are based on equations that have been experimentally verified. Therefore, these equations should prove to be a valuable tool for aiding an LV user in proper system alignment and assessing the measurement capabilities of the system.

Acknowledgments

This work was performed under the auspices of Grant NGT-50868 provided through the NASA Langley Research Center, while the first author was in residence at West Virginia University. The authors wish to thank James F. Meyers for suggesting the research presented in this paper.

References

[1]Hanson, S., "Broadening of the Measured Frequency Spectrum in a Differential Laser Anemometer due to Interference Plane Gradients," *Journal of Physics D—Applied Physics,* Vol. 6, No. 2, 1973, pp. 164–171.

[2]Durst, F., and Stevenson, W. H., "Properties of Focused Laser Beams and the Influence on Optical Anemometer Signals," *Proceedings—Minnesota Symposium on Laser Anemometry* (Oct. 1975), edited by E. R. G. Eckert, University of Minnesota, Minneapolis, MN, 1976, pp. 371–387.

[3]Anon., *55X Modular LDA Optics Manual,* DISA/Dantec Elektronik, DISA Information Dept. Scientific Research Equipment Div. Reg. No. 9150A7512, Skovlunde, Denmark, Aug. 1984, p. 17.

[4]Fleming, G. A., "Error Analyses of Laser Velocimetry Measurements," MSME Thesis, Department of Mechanical and Aerospace Engineering, West Virginia University, Morgantown, WV, May 1993.